

Asymmetric Distribution of Primary Cilia Allocates Satellite Cells for Self-Renewal

Nur Hayati Jaafar Marican,¹ Sara B. Cruz-Migoni,¹ and Anne-Gaëlle Borycki^{1,*}

¹Department of Biomedical Science, University of Sheffield, Firth Court, Western Bank, Sheffield S10 2TN, UK

*Correspondence: a.g.borycki@sheffield.ac.uk

<http://dx.doi.org/10.1016/j.stemcr.2016.04.004>

SUMMARY

Regeneration of vertebrate skeletal muscles requires satellite cells, a population of stem cells that are quiescent in normal conditions and divide, differentiate, and self-renew upon activation triggered by exercise, injury, and degenerative diseases. Satellite cell self-renewal is essential for long-term tissue homeostasis, and previous work has identified a number of external cues that control this process. However, little is known of the possible intrinsic control mechanisms of satellite cell self-renewal. Here, we show that quiescent satellite cells harbor a primary cilium, which is rapidly disassembled upon entry into the cell cycle. Contrasting with a commonly accepted belief, cilia reassembly does not occur uniformly in cells exiting the cell cycle. We found that primary cilia reassemble preferentially in cells committed to self-renew, and disruption of cilia reassembly causes a specific deficit in self-renewing satellite cells. These observations indicate that primary cilia provide an intrinsic cue essential for satellite cell self-renewal.

INTRODUCTION

Vertebrate skeletal muscles are self-renewing organs that rely on the activity of muscle-specific stem cells, named satellite cells (SCs), to maintain a balance between the production of muscle progenitor cells that differentiate to repair muscles and the generation of self-renewing cells that maintain a pool of “reserve cells” for future requirement. Reserve satellite cells can be produced from activated SCs via one of two mechanisms: symmetric cell division, which generates two identical daughter stem cells, and asymmetric cell division, which generates two daughter cells with distinct fates (Dumont et al., 2015). Under normal demand, reserve cells are primarily produced via asymmetric cell division, whereas under extreme circumstances they are produced via symmetric cell division. Understanding the cues and molecular mechanisms that regulate satellite cell self-renewal is critical, as disruption in the balance that controls the number of muscle progenitor cells and reserve cells has profound consequences for the regenerative capability of skeletal muscles and underpins the reduced muscle mass (sarcopenia) in aged muscles (Chakkalakal et al., 2012; Conboy and Rando, 2005).

SC self-renewal through symmetric cell division occurs mostly in the planar orientation (parallel to the fiber) and involves the planar cell polarity pathway (Le Grand et al., 2009). Conversely, asymmetric SC cell division occurs primarily along the apicobasal axis and generates a self-renewing daughter cell associated with the basal lamina that covers the muscle fiber and a differentiating daughter cell that faces the sarcolemma (Kuang et al., 2007). Both intrinsic and extrinsic cues regulate SC asymmetric cell di-

vision. However, while an important focus has been placed on extrinsic factors controlling SC asymmetric cell division (Conboy and Rando, 2002; Urciolo et al., 2013), intrinsic cues have only begun to be elucidated. These include the asymmetric distribution of cytoplasmic and nuclear fate determinants (Gopinath et al., 2014; Le Grand et al., 2012; Shea et al., 2010) and/or the asymmetric inheritance of template DNA (Rocheteau et al., 2012; Shinin et al., 2006). Both mechanisms rely on the polarity of dividing SCs, which is established by the activity of the PAR complex and influences the orientation of mitotic spindles (Troy et al., 2012; Williams and Fuchs, 2013). Centrosomes play a key role in this process as microtubule organizing centers, and previous studies have reported that the asymmetric segregation of the mother and daughter centrioles during mitotic spindle formation confers differential cell-fate cues (Pelletier and Yamashita, 2012). The mother centriole acts also as a nucleating center for the formation of primary cilia, a cellular organelle anchored in the cytoplasm through a basal body composed of the mother centriole and protruding outside the cell through a microtubule-containing appendage (Kim and Dynlacht, 2013). Given these facts, we asked whether primary cilia play a role in SC self-renewal.

Here, we show that quiescent SCs contain a primary cilium, which disassembles upon SC activation and entry into the cell cycle. Upon exit from the cell cycle, primary cilia reassemble at the surface of a minority of SCs, which are fated to self-renew. Disruption of cilia reassembly following cell division drives muscle progenitor cells toward differentiation, at the expense of self-renewal. Thus, our work demonstrates that the primary cilium is an intrinsic cue that determines the self-renewal fate in SCs.

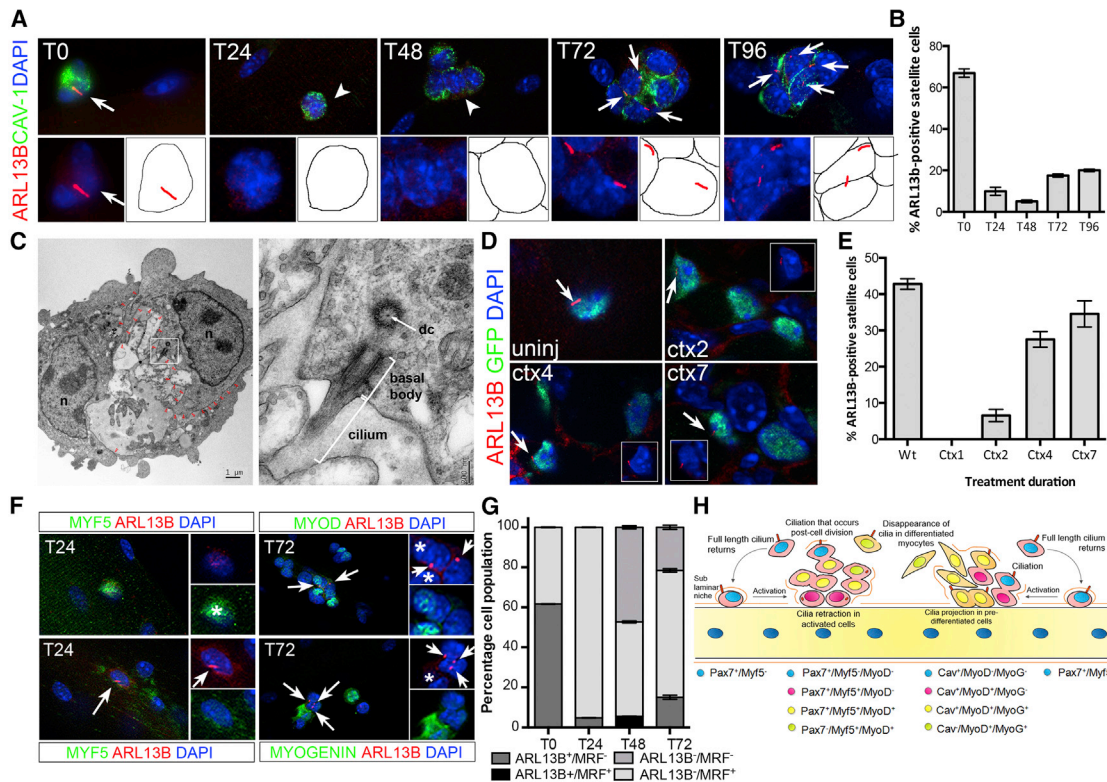


Figure 1. Primary Cilia Are Predominantly Observed at the Surface of Quiescent Satellite Cells

(A) ARL13B (red) in SCs (caveolin-1, CAV-1, green) from C57BL/6 EDL myofibers cultured for 96 hr. White arrows indicate the presence of primary cilia at the surface of SCs. White arrowheads indicate cells lacking cilia.

(B) Percentage of SCs bearing a primary cilium during the 96-hr myofiber culture. $n = 50$ fibers per time point from five independent experiments. Mean \pm SEM is shown.

(C) Transmitted electron microscopy of SCs following a 72-hr culture of C57BL/6 myofibers. The left panel shows two satellite cells following cell division (scale bar, 1 μ m). The right panel is a high magnification of the area indicated by a white box showing a primary cilium (scale bar, 200 nm). n, nucleus; dc, daughter centriole; open red arrowheads mark the SC cell surface.

(D) Detection of ARL13B (red) at the surface of SCs in cardiotoxin-injured TA muscles of *Tg(Pax7-GFP)* mice at 2, 4, and 7 days post injury. Control is uninjured (uninj) *Tg(Pax7-GFP)* TA muscle. White arrows indicate primary cilia. Insets show the red and blue channel images of the cell indicated by white arrows.

(E) Quantification of data presented in (D) showing the percentage of GFP-labeled SCs bearing a primary cilium in injured muscles. Mean \pm SEM is shown. 4–8 sections were analyzed from three mice per time point.

(F) Immunofluorescence analysis of primary cilia (ARL13B; red) and myogenic regulatory factors (Mrf) MYF5 (green at T24), MYOD (green at T72), and MYOGENIN (green at T72). White arrows indicate primary cilia. White stars indicate Mrf-positive cells that lack cilia.

(G) Freshly isolated 24-, 48-, and 72-hr cultured myofibers analyzed by immunofluorescence using antibodies against ARL13B and MYF5 (24 hr), MYOD (48 hr), and MYOGENIN (72 hr). M-CADHERIN was used as an SC marker. The percentage of MYF5/MYOD/MYOGENIN-labeled cells (Mrf⁺) containing a primary cilium (black bars) or not (gray bars) was scored. $n = 50$ myofibers analyzed per time point from three independent experiments; mean \pm SEM is shown.

(H) Graphical representation of cilia dynamics during adult myogenesis.

See also Figure S1.

RESULTS

Primary Cilia Are Predominantly Observed at the Surface of Quiescent Satellite Cells

Skeletal muscle fibers extracted from extensor digitorum longus (EDL) muscles of C57BL/6 mice were cultured for 96 hr. Under these conditions, SCs are in their native envi-

ronment and are immunodetected with antibodies against caveolin-1 (CAV-1) (Figure 1A). Using antibodies directed against ADP-ribosylation factor-like 13b (ARL13B), a small guanosine triphosphatase specific to the ciliary membrane, we observed the presence of primary cilia in 67% of SCs from freshly isolated myofibers (T0, Figures 1A and 1B). Primary cilia were also labeled by acetylated α -TUBULIN



(Figure S1A). Transmission electron microscopy of myofibers cultured for 72 hr (T72) confirmed that the structure labeled with ARL13B and acetylated α -TUBULIN has a 9 + 0 configuration consistent with a primary cilium (Figure 1C). The average length of cilia on quiescent SCs was 2.74 μm (n = 20; SD = 0.23), a length similar to that of 10T1/2 fibroblasts (2.86 μm) (Bershteyn et al., 2010). Within 24 hr (T24), when SCs exit quiescence, become activated, and express MYF5, only a small proportion of SCs exhibited cilia (9.9%, Figures 1A and 1B). Cilia numbers continued to decrease in 48-hr culture (T48) SCs, which express MYOD and proliferate to yield transit-amplifying cells (Figures 1A and 1B). However, at 72 hr (T72) when satellite cells either downregulate PAX7 and activate MYOGENIN to differentiate, or maintain PAX7 and return to quiescence to self-renew, we observed that cilia reappeared in about 17% of SCs (Figures 1A and 1B). We examined myofibers at 96 hr (T96) to test whether additional primary cilia were generated (Anderson and Stearns, 2009). We noticed no significant increase in the percentage of ARL13B-positive SCs (Figures 1A and 1B). Thus, the small proportion of SCs harboring a primary cilium at T72 and T96 defined a specific cell population.

We next asked whether primary cilia were present at the surface of SCs in vivo. The tibialis anterior (TA) muscle of *Tg(Pax7-GFP)* mice, which express GFP under the control of the SC-specific *Pax7* promoter, was injured by cardiotoxin injection and muscle regeneration monitored at 1, 2, 4, and 7 days post injury. Primary cilia were detected at the surface of quiescent SCs in non-injured muscles, but not in activated SCs at 1 day post injury (Figures 1D and 1E). Cilia reassembly initiated in muscles at 2 days post injury and continued until 7 days post injury (Figures 1D and 1E). Therefore, primary cilia are predominantly associated with quiescent SCs and dissociate at the onset of muscle injury in activated SCs, but reassemble in a subset of Pax7-expressing cells as muscles repair (Figures 1D and 1E). As ARL13B and MYF5, a marker of activated SCs, were mutually exclusive in freshly isolated and in T24 SCs (Figures 1F and 1G), we performed a time-course analysis of primary cilia disassembly. This showed that primary cilia dissociation initiates as early as 4 hr after plating myofibers, and by 12 hr primary cilia are fully resorbed (Figure S1B). Strangely, at T48 a small proportion of MYOD⁺ SCs possessed a primary cilium (Figure 1G). However, a detailed time-course analysis of primary cilium dynamics between T48 and T72 confirmed that the co-detection of MYOD and primary cilium was transient and that by 60 hr of culture MYOD and ARL13B are mutually exclusive in SCs (Figure S1C). We also observe that by 72 hr in culture, the only ARL13B⁺ SCs present were MYOD⁻ and MYOGENIN⁻ (Figures 1F and 1G), suggesting that the reassembly of primary cilia post cell division occurs in self-re-

newing SCs. Thus, primary cilia are regulated in a highly dynamic manner during adult myogenesis with a rapid dissociation within a few hours after SC activation and the subsequent reassembly in a subset of SCs that appear fated to self-renew (Figure 1H).

Cell-Cycle Entry Initiates Primary Cilia Disassembly in Satellite Cells

The kinetics of primary cilium distribution during myogenesis suggests a mutually exclusive relationship between cilia and cell cycle. Myoblast cell-cycle progression through G1/S transition is controlled by cyclin-dependent kinase 4/6 (Saab et al., 2006). Thus, we treated cultured myofibers with a CDK4/6 inhibitor, which blocked SCs in G1 (Figures 2A–2C). Cell-cycle arrest was accompanied with the maintenance of primary cilia (Figures 2B and 2C). When CDK4/6 inhibition was reversed and SCs allowed to re-enter the cell cycle, primary cilia disassembled by 72 hr (Figures 2D–2F), reinforcing our conclusion that primary cilium turnover in cultured myofibers is directly linked to and mutually exclusive with SC entry into the cell cycle.

Primary Cilia Are Preferentially Associated with Satellite Cells Engaged in Self-Renewal

Given that primary cilia are resorbed in dividing SCs and not detected in activated (MYF5⁺) or differentiating (MYOGENIN⁺) cells, we reasoned that primary cilia may be associated with self-renewing SCs. We thus analyzed the distribution and plan of division of cilia-bearing cells at T48 and T72. At T48, the majority of cell doublets analyzed (79.8%) do not harbor a primary cilium. Of the remaining doublets presenting cilia (20.2%), 26% of doublets displayed an asymmetric distribution of their primary cilia with no bias for the division plan. The remaining doublets with a symmetrical distribution of cilia were mainly undergoing planar cell division (65.5%) (Figures 3A and 3B). At T72, about half of cell doublets were associated with at least one primary cilium, which were largely distributed asymmetrically (96% of ARL13B⁺ doublets) either in planar cell division (34% of ARL13B⁺ doublets) or in apicobasal cell division (62% of ARL13B⁺ doublets) events (Figures 3A and 3B). Furthermore, the primary cilium was invariably observed in the daughter cell associated with the basal lamina in cell divisions with an apicobasal orientation (Figures 3A and 3B). Thus, when SCs are proliferating to produce transit-amplifying cells (at T48), primary cilia are mainly distributed symmetrically and are associated with both planar and apicobasal cell-division events. By T72 when a subset of progenitor cells commit to self-renewal, primary cilia become asymmetrically distributed and are mainly associated with apicobasal cell-division events. Given that self-renewing SCs downregulate MYOD, fail to activate MYOGENIN, and instead maintain PAX7 expression, we

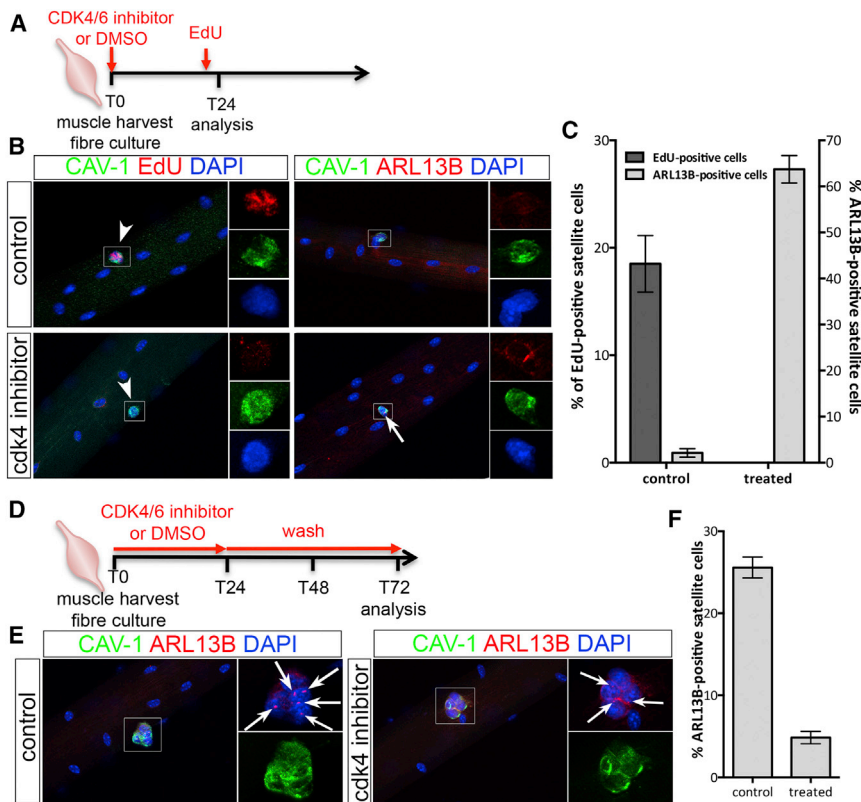


Figure 2. Cilia Dynamic Is Associated with the Cell Cycle in Satellite Cells

(A) Schematic representation of the experimental design used in (B) and (C).

(B) Representative images of EDL myofibers cultured for 24 hr in the presence or not of CDK4/6 kinase inhibitor and analyzed for either the inhibition of cell-cycle progression (EdU incorporation in red) or the presence of primary cilia (ARL13B in red). White arrows indicate the presence of cilia. White arrowheads indicate SCs. Insets show higher magnification images of the area indicated by a white rectangle in each color channel.

(C) Percentage of SCs engaged in the cell cycle (EdU⁺ in dark gray) and exhibiting a primary cilium (ARL13B⁺ in light gray) following a 24-hr culture in control (DMSO) or in treated conditions (CDK4/6 inhibitor). n = 50 fibers analyzed per condition from three independent experiments; mean ± SEM is shown.

(D) Schematic representation of the experimental design used in (E) and (F).

(E) Representative images of myofibers after a 72-hr culture in control conditions (left panels) or following a 24-hr CDK4/6 inhibitor treatment and a 2-day wash in

normal medium (right panels). White arrows indicate the presence of primary cilia (labeled with ARL13B in red). Insets show higher magnification images of the area indicated by a white rectangle in the red and blue, and green channels.

(F) Percentage of SCs exhibiting a primary cilium in control or treated conditions. n = 50 fibers analyzed per condition from three independent experiments; mean ± SEM is shown.

first examined whether the asymmetric distribution of primary cilia at T72 correlated with a self-renewing cell fate. Consistent with our observations that MYOD-expressing and MYOGENIN-expressing cells did not harbor a primary cilium at T72 (Figures 1F and 1G), we found that ARL13B co-localized with approximately 15% of GFP-positive cells and was mutually exclusive with MYOGENIN in T72 myofiber cultures from *Tg(Pax7-GFP)* muscles (Figures 3C and 3D). Furthermore, the analysis of the distribution of primary cilia (ARL13B⁺) in ciliated doublets at T72 revealed that primary cilia were mainly asymmetrically allocated to self-renewing cells or cells deemed to self-renew (PAX7/GFP⁺MYOGENIN⁻) following apicobasal cell division (Figure 3E). Together, our observations suggest that the reassembly of primary cilia after cell division occurs preferentially in daughter cells that underwent asymmetric cell division and are fated to self-renew.

Disruption of Cilia Reassembly Impairs Satellite Cell Self-Renewal

We next asked whether cilia reassembly following SC asymmetric cell division was essential for SC self-renewal. Myo-

fibers cultured for 66 hr to allow for cell division were treated with nocodazole or taxol, which affect cilia by destabilizing microtubule or by altering the levels of soluble tubulin, respectively (Sharma et al., 2011), or with forchlorfenuron (FCF), an inhibitor of Septins, a family of proteins that regulate cilia length and stability (Zhai et al., 2014), and cultured for a further 6 hr before analysis at T72 (Figure 4A). At T72, nocodazole or taxol treatment caused 100% inhibition, whereas FCF caused 58% inhibition of cilia reassembly (Figure 4B). The proportion of 5-ethynyl-2'-deoxyuridine (EdU)-labeled SCs was similar between nocodazole or FCF-treated cultures and control (DMSO-treated) cultures (Figure 4C), confirming that a short treatment has little or no impact on the cell cycle. However, nocodazole, taxol, and FCF treatment caused a decrease in the number of PAX7⁺MYOGENIN⁻M-CADHERIN⁺ SCs, which labels self-renewing cells, and a concomitant increase in the number of Pax7⁻MYOGENIN⁺M-CADHERIN⁺ SCs, which labels differentiating cells (Figures 4D and 4E). Consistent with the partial loss of primary cilia upon FCF treatment, a somewhat lesser effect on self-renewing SCs was observed in FCF-treated myofibers (Figure 4E). Thus,

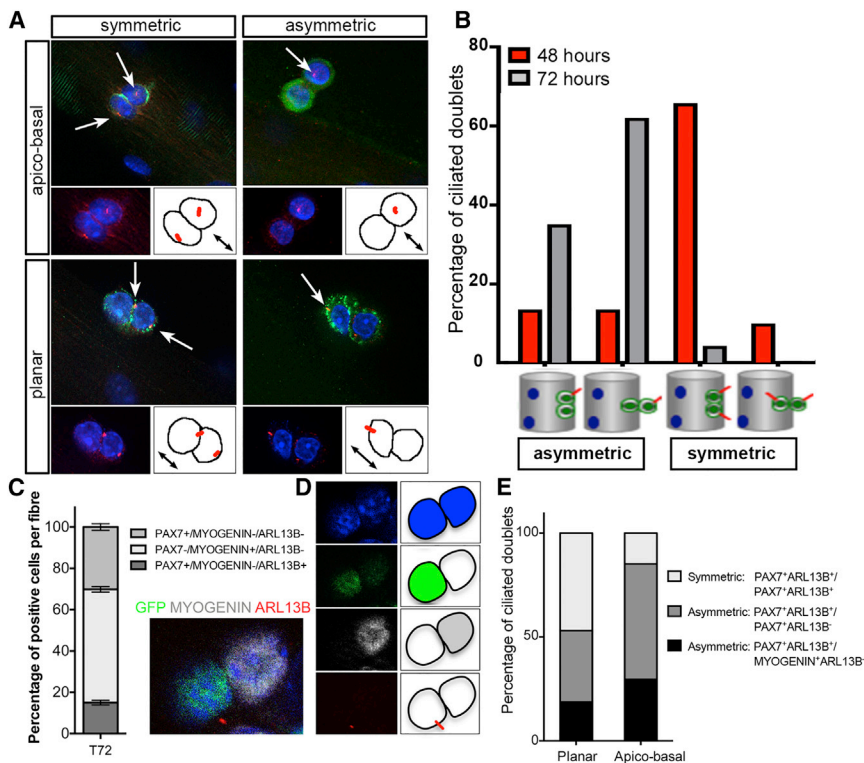


Figure 3. Primary Cilia Are Preferentially Associated with Satellite Cells Engaged in Self-Renewal

(A) Representative images of cilia distribution (symmetric or asymmetric) at the surface of SCs undergoing apicobasal (perpendicular to the myofiber axis) or planar (parallel to the myofiber axis) cell division (CAV-1 in green, ARL13B in red, and DAPI in blue). White arrows indicate the presence of primary cilia. Black arrows indicate the axis of the myofiber.

(B) Quantification of primary cilia distribution at the surface of dividing SCs after 48 (red bars) and 72 (gray bars) hr in culture. Symmetric and asymmetric cilia distribution in cell doublets undergoing planar or apicobasal cell division was scored and the percentage of each event among cilia-bearing doublets was plotted. Note that at 72 hr cilia are primarily asymmetrically distributed in SCs, whereas a symmetric distribution is observed at 48 hr. A total of 114 (48 hr) and 56 (72 hr) doublets were examined (n = 2 experiments), of which 20.2% (48 hr) and 50% (72 hr) harbored at least one cilium.

(C) Quantification of the percentage of positive SCs following triple immunolabeling with antibodies against GFP (PAX7; green), MYOGENIN (white), and ARL13B (red) in myofibers isolated from *Tg(Pax7-GFP)* EDL muscles and cultured for 72 hr. n = 49 fibers from four independent experiments.

(D) Representative images of SCs quantified in (E) showing that ARL13B (red) is mutually exclusive with MYOGENIN (white) and always associated with GFP (PAX7; green). Images in the blue, green, red, and white channels, as well as the merge image, are shown.

(E) Percentage of ciliated doublets associated with planar or apicobasal cell divisions in *Tg(Pax7-GFP)* myofibers cultured for 72 hr. The distribution of primary cilia (ARL13B⁺), symmetric or asymmetric, within doublets and co-localization with PAX7/GFP and MYOGENIN was determined. Note that while asymmetric cell divisions resulting in distinct cell fates in daughter cells (MYOGENIN⁺ versus PAX7/GFP⁺) represent about 19% of planar cell divisions, they account for nearly 29% of apicobasal cell divisions. n = 32 planar doublets and n = 27 apicobasal doublets from two independent experiments.

blocking primary cilium reassembly following cell division disrupts the balance between differentiation and self-renewal, and impairs SC self-renewal at the expense of differentiation. This suggests that the selective reassembly of a primary cilium at the surface of one daughter cell, following asymmetric cell division, allocates SCs to a self-renewing cell fate.

DISCUSSION

The primary cilium is a microtubule-containing cellular protrusion, which is anchored to a basal body constituted of a mother centriole acting as a microtubule organizing center during ciliogenesis (Kim and Dynlacht, 2013). Thus, it is widely accepted that primary cilia must dissociate prior to mitosis to release the centrioles for their sub-

sequent enrolment in mitotic spindle formation and that primary cilia reassemble following cell division (Nigg and Stearns, 2011). Here, we showed that quiescent SCs harbor a primary cilium, which resorbs rapidly upon SC activation and entry into the cell cycle, before reassembling asymmetrically following apicobasal cell division in cells associated with the basal lamina. Furthermore, we found that primary cilium reassembly occurs preferentially in daughter stem cells. Previous studies reported the asymmetric inheritance of the mother centriole by self-renewing radial glial cells in the neocortex, whereas cells inheriting the daughter centriole differentiated (Wang et al., 2009). Given that the mother centriole plays a key role in primary cilium assembly (Kim and Dynlacht, 2013), it can be expected that primary cilia reassemble exclusively in self-renewing cells. Consistent with our findings, Paridaen et al. (2013) reported the selective retention of the ciliary membrane in

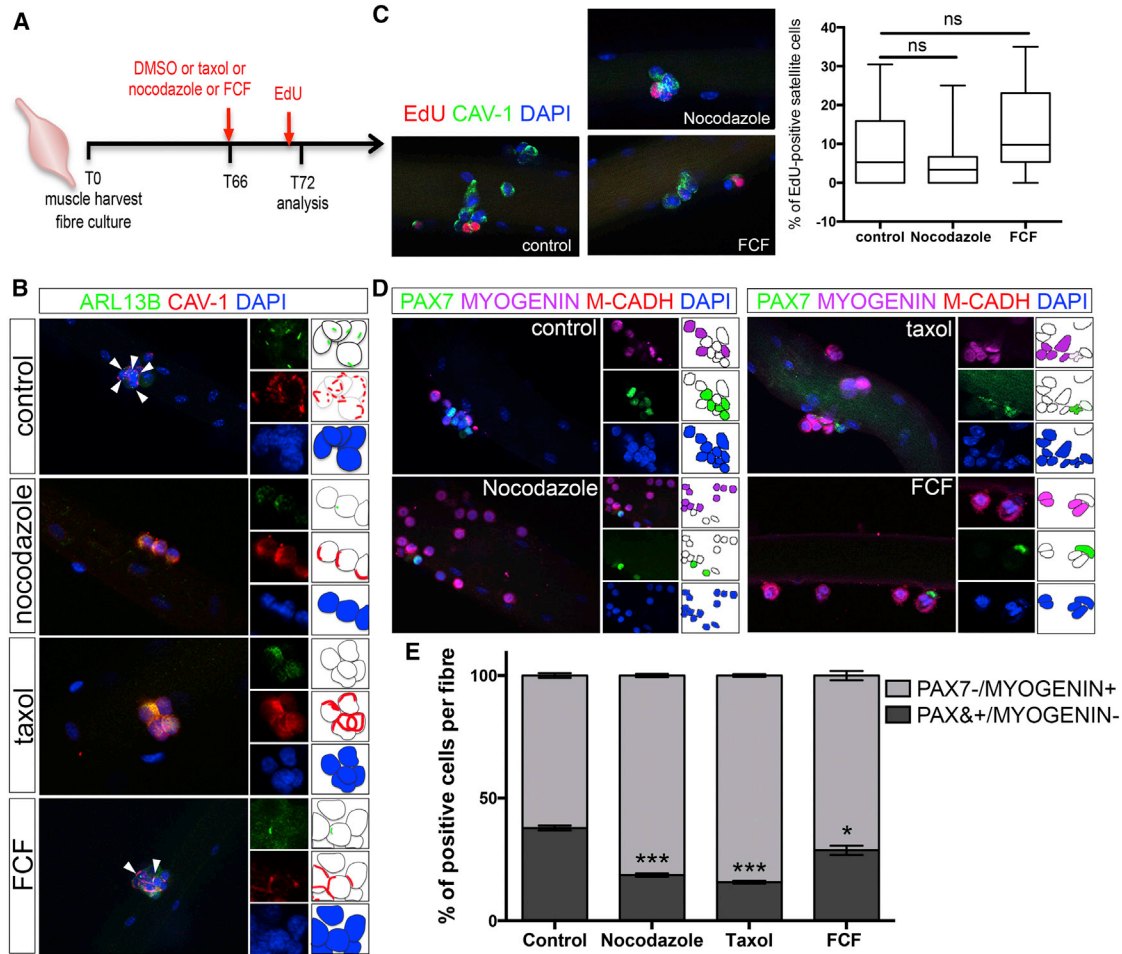


Figure 4. Disruption of Cilia Reassembly Impairs Satellite Cell Self-Renewal

(A) Schematic representation of the experimental design used in (B–E).

(B) Representative images of EDL T72 myofiber cultures treated with DMSO (control), taxol (2 μ M), nocodazole (4 μ M), or forchlorfenuron (FCF, 10 μ M) at T66, and analyzed by immunofluorescence for the presence of primary cilia (ARL13B; green) in SCs (CAVEOLIN-1, red). White arrowheads indicate the presence of cilia.

(C) Representative images of EDL myofibers cultured in the presence of DMSO (control) or nocodazole or FCF and analyzed for the incorporation of EdU. A graph shows the percentage of EdU-positive cells per myofiber in each culture condition. n = 18–23 fibers. ns, not significant.

(D) Representative images of EDL myofibers cultured in the presence of DMSO (control), nocodazole, taxol, or FCF and analyzed by immunofluorescence using antibodies against PAX7 (green), MYOGENIN (magenta), and M-CADHERIN (red). Nuclei were counterstained with DAPI (blue).

(E) Percentage of cells observed in control cultures and in cultures following treatment with taxol, nocodazole, and FCF. Note that self-renewing SCs are PAX7⁺/MYOGENIN⁻ (dark gray). n = 50–85 fibers from three independent experiments analyzed per condition; mean \pm SEM is shown. ***p < 0.0001, *p < 0.05.

neural stem cells that inherited the mother centriole. Interestingly, the simultaneous transmission of the mother centriole associated with ciliary membrane remnant conferred a temporal advantage, as the primary cilium was found to reassemble more rapidly in self-renewing daughter cells than in differentiating daughter cells. Despite extending the myofiber culture period to 96 hr, we did not observe an increased number of muscle progen-

itor cells presenting a primary cilium. This suggests that in contrast to neural stem cells, asymmetric SC cell division did not generate differential ciliogenesis kinetics but led to the selective reassembly of the primary cilium in daughter stem cells in skeletal muscles. Moreover, preventing primary cilium reassembly impaired SCs' ability to self-renew and drove SCs to differentiation, indicating that the primary cilium functions in SC cell-fate decision



and is an essential intrinsic cue required for SC self-renewal. Given that primary cilia are cellular appendages that regulate a number of signaling pathways, including SHH, WNT, PDGF, and HIPPO (Basten and Giles, 2013), one may speculate that the preferential reassembly of primary cilia in self-renewing daughter cells favors cell signaling for the induction of the self-renewal cell fate. In the neuroepithelium of developing mouse embryos, the asynchronous reassembly of primary cilia in daughter cells is associated with differential SHH response (Piotrowska-Nitsche and Caspary, 2012). Although the evidence of a similar involvement of SHH signaling in SC self-renewal is still lacking, SHH response was shown to correlate with the presence of primary cilia in differentiating myogenic cell lines (Fu et al., 2014). Also of interest is the role of the primary cilium in the control of endogenous β -catenin levels and the balance between canonical and non-canonical WNT signaling (Corbit et al., 2008; Lancaster et al., 2011), as these pathways are implicated in SC growth and self-renewal, respectively (Le Grand et al., 2009; Otto et al., 2008). Future studies will determine whether the primary cilium controls SC self-renewal by regulating the availability of signaling pathway components.

EXPERIMENTAL PROCEDURES

Experimental animal work was carried out under a UK Home Office Licence in accordance with the 1986 UK Animal Act.

Mice and Muscle Injury

Tg(Pax7-GFP) and C57BL/6 mice were bred in-house and PCR genotyped as described previously (Sambasivan et al., 2009). Mice were anesthetized by isoflurane inhalation and 50 μ l of cardiotoxin (10 μ M, Latoxan) was injected into the right TA muscle. The contralateral untreated TA muscle served as the control.

Single Myofiber Isolation and Culture

Single myofibers were isolated from the EDL muscle of 8- to 10-week-old C57BL/6 mice after digestion with collagenase A (Sigma) as previously described (Collins and Zammit, 2009). Isolated myofibers were fixed in 4% paraformaldehyde (PFA; BDH Laboratory Supplies) for 8 min at room temperature and washed extensively in 1 \times PBS (Fisher Scientific) or cultured in 5% BSA (Sigma)-coated plates containing DMEM (Glutamax; Gibco) supplemented with 10% horse serum (Gibco), 1% penicillin-streptomycin-fungizone (Gibco), and 0.5% chicken embryo extract (Serlab) for 24, 48, 72, and 96 hr. Following culture, myofibers were harvested and fixed in 4% PFA.

Click-iT EdU Labeling

DNA synthesis was directly measured using Click-iT EdU imaging kit (Invitrogen) according to the manufacturer's protocol (Life Technologies). EdU was added to myofiber cultures 1 hr prior to harvesting.

Additional methods are provided in [Supplemental Experimental Procedures](#).

SUPPLEMENTAL INFORMATION

Supplemental Information includes Supplemental Experimental Procedures, one figure, and one table and can be found with this article online at <http://dx.doi.org/10.1016/j.stemcr.2016.04.004>.

ACKNOWLEDGMENTS

We are indebted to Prof. Shahragim Tajbakhsh for providing us with the *Tg(Pax7-GFP)* mice. We wish to thank staff at the Biological Service Unit for their excellent technical support, Kamalliawati Mohd Imran for her assistance, and members of the laboratory for discussions. Monoclonal antibodies reported in this study were obtained from the Developmental Studies Hybridoma Bank developed under the auspices of the NICHD and maintained by the Department of Biology, University of Iowa. This work was supported by grants from the Association Francaise contre les Myopathies.

Received: June 9, 2015

Revised: April 5, 2016

Accepted: April 5, 2016

Published: May 5, 2016

REFERENCES

- Anderson, C.T., and Stearns, T. (2009). Centriole age underlies asynchronous primary cilium growth in mammalian cells. *Curr. Biol.* *19*, 1498–1502.
- Basten, S.G., and Giles, R.H. (2013). Functional aspects of primary cilia in signaling, cell cycle and tumorigenesis. *Cilia* *2*, 6.
- Bershteyn, M., Atwood, S.X., Woo, W.M., Li, M., and Oro, A.E. (2010). MIM and cortactin antagonism regulates ciliogenesis and hedgehog signaling. *Dev. Cell* *19*, 270–283.
- Chakkalakal, J.V., Jones, K.M., Basson, M.A., and Brack, A.S. (2012). The aged niche disrupts muscle stem cell quiescence. *Nature* *490*, 355–360.
- Collins, C.A., and Zammit, P.S. (2009). Isolation and grafting of single muscle fibres. *Methods Mol. Biol.* *482*, 319–330.
- Conboy, I.M., and Rando, T.A. (2002). The regulation of Notch signaling controls satellite cell activation and cell fate determination in postnatal myogenesis. *Dev. Cell* *3*, 397–409.
- Conboy, I.M., and Rando, T.A. (2005). Aging, stem cells and tissue regeneration: lessons from muscle. *Cell Cycle* *4*, 407–410.
- Corbit, K.C., Shyer, A.E., Dowdle, W.E., Gaulden, J., Singla, V., Chen, M.H., Chuang, P.T., and Reiter, J.F. (2008). Kif3a constrains beta-catenin-dependent Wnt signalling through dual ciliary and non-ciliary mechanisms. *Nat. Cell Biol.* *10*, 70–76.
- Dumont, N.A., Wang, Y.X., and Rudnicki, M.A. (2015). Intrinsic and extrinsic mechanisms regulating satellite cell function. *Development* *142*, 1572–1581.
- Fu, W., Asp, P., Canter, B., and Dynlacht, B.D. (2014). Primary cilia control hedgehog signaling during muscle differentiation and are



- deregulated in rhabdomyosarcoma. *Proc. Natl. Acad. Sci. USA* *111*, 9151–9156.
- Gopinath, S.D., Webb, A.E., Brunet, A., and Rando, T.A. (2014). FOXO3 promotes quiescence in adult muscle stem cells during the process of self-renewal. *Stem Cell Rep.* *2*, 414–426.
- Kim, S., and Dynlacht, B.D. (2013). Assembling a primary cilium. *Curr. Opin. Cell Biol.* *25*, 506–511.
- Kuang, S., Kuroda, K., Le Grand, F., and Rudnicki, M.A. (2007). Asymmetric self-renewal and commitment of satellite stem cells in muscle. *Cell* *129*, 999–1010.
- Lancaster, M.A., Schroth, J., and Gleeson, J.G. (2011). Subcellular spatial regulation of canonical Wnt signalling at the primary cilium. *Nat. Cell Biol.* *13*, 700–707.
- Le Grand, F., Jones, A.E., Seale, V., Scime, A., and Rudnicki, M.A. (2009). Wnt7a activates the planar cell polarity pathway to drive the symmetric expansion of satellite stem cells. *Cell Stem Cell* *4*, 535–547.
- Le Grand, F., Grifone, R., Mourikis, P., Houbron, C., Gigaud, C., Pujol, J., Maillat, M., Pages, G., Rudnicki, M., Tajbakhsh, S., et al. (2012). Six1 regulates stem cell repair potential and self-renewal during skeletal muscle regeneration. *J. Cell Biol.* *198*, 815–832.
- Nigg, E.A., and Stearns, T. (2011). The centrosome cycle: centriole biogenesis, duplication and inherent asymmetries. *Nat. Cell Biol.* *13*, 1154–1160.
- Otto, A., Schmidt, C., Luke, G., Allen, S., Valasek, P., Muntoni, F., Lawrence-Watt, D., and Patel, K. (2008). Canonical Wnt signalling induces satellite-cell proliferation during adult skeletal muscle regeneration. *J. Cell Sci.* *121*, 2939–2950.
- Paridaen, J.T., Wilsch-Brauninger, M., and Huttner, W.B. (2013). Asymmetric inheritance of centrosome-associated primary cilium membrane directs ciliogenesis after cell division. *Cell* *155*, 333–344.
- Pelletier, L., and Yamashita, Y.M. (2012). Centrosome asymmetry and inheritance during animal development. *Curr. Opin. Cell Biol.* *24*, 541–546.
- Piotrowska-Nitsche, K., and Caspary, T. (2012). Live imaging of individual cell divisions in mouse neuroepithelium shows asymmetry in cilium formation and Sonic hedgehog response. *Cilia* *1*, 6.
- Rocheteau, P., Gayraud-Morel, B., Siegl-Cachedenier, I., Blasco, M.A., and Tajbakhsh, S. (2012). A subpopulation of adult skeletal muscle stem cells retains all template DNA strands after cell division. *Cell* *148*, 112–125.
- Saab, R., Bills, J.L., Miceli, A.P., Anderson, C.M., Khoury, J.D., Fry, D.W., Navid, F., Houghton, P.J., and Skapek, S.X. (2006). Pharmacologic inhibition of cyclin-dependent kinase 4/6 activity arrests proliferation in myoblasts and rhabdomyosarcoma-derived cells. *Mol. Cancer Ther.* *5*, 1299–1308.
- Sambasivan, R., Gayraud-Morel, B., Dumas, G., Cimper, C., Paisant, S., Kelly, R.G., and Tajbakhsh, S. (2009). Distinct regulatory cascades govern extraocular and pharyngeal arch muscle progenitor cell fates. *Dev. Cell* *16*, 810–821.
- Sharma, N., Kosan, Z.A., Stallworth, J.E., Berbari, N.F., and Yoder, B.K. (2011). Soluble levels of cytosolic tubulin regulate ciliary length control. *Mol. Biol. Cell* *22*, 806–816.
- Shea, K.L., Xiang, W., LaPorta, V.S., Licht, J.D., Keller, C., Basson, M.A., and Brack, A.S. (2010). Sprouty1 regulates reversible quiescence of a self-renewing adult muscle stem cell pool during regeneration. *Cell Stem Cell* *6*, 117–129.
- Shinin, V., Gayraud-Morel, B., Gomes, D., and Tajbakhsh, S. (2006). Asymmetric division and cosegregation of template DNA strands in adult muscle satellite cells. *Nat. Cell Biol.* *8*, 677–687.
- Troy, A., Cadwallader, A.B., Fedorov, Y., Tyner, K., Tanaka, K.K., and Olwin, B.B. (2012). Coordination of satellite cell activation and self-renewal by Par-complex-dependent asymmetric activation of p38alpha/beta MAPK. *Cell Stem Cell* *11*, 541–553.
- Urciuolo, A., Quarta, M., Morbidoni, V., Gattazzo, F., Molon, S., Grumati, P., Montemurro, F., Tedesco, F.S., Blaauw, B., Cossu, G., et al. (2013). Collagen VI regulates satellite cell self-renewal and muscle regeneration. *Nat. Commun.* *4*, 1964.
- Wang, X., Tsai, J.W., Imai, J.H., Lian, W.N., Vallee, R.B., and Shi, S.H. (2009). Asymmetric centrosome inheritance maintains neural progenitors in the neocortex. *Nature* *461*, 947–955.
- Williams, S.E., and Fuchs, E. (2013). Oriented divisions, fate decisions. *Curr. Opin. Cell Biol.* *25*, 749–758.
- Zhai, G., Gu, Q., He, J., Lou, Q., Chen, X., Jin, X., Bi, E., and Yin, Z. (2014). Sept6 is required for ciliogenesis in Kupffer's vesicle, the pronephros, and the neural tube during early embryonic development. *Mol. Cell Biol.* *34*, 1310–1321.

Stem Cell Reports, Volume 6

Supplemental Information

**Asymmetric Distribution of Primary Cilia Allocates Satellite Cells for
Self-Renewal**

Nur Hayati Jaafar Marican, Sara B. Cruz-Migoni, and Anne-Gaëlle Borycki

Supplemental Information

Experimental Procedures

Drug treatment

CDK4/6 inhibitor (PD0332991 isothionate; Sigma) was used to induce G1-cell cycle arrest. A dose-response curve was first established to determine the concentration required to block cell cycle progression. Thereafter, myofibers were treated with 750nM CDK4/6 inhibitor for 24 hours or for 24 hours followed by 48 hours in normal culture medium. Control myofibers were supplemented with 0.1% DMSO (Sigma). Taxol (2 μ M; Sigma) and Nocodazole (4 μ M; Sigma) were used at concentrations previously reported to block microtubules/cilia reassembly (Sharma et al., 2011). Forchlorfenuron (FCF; Sigma), diluted in DMSO, was tested on myofiber cultures at concentrations varying from 10 μ M to 100 μ M. A concentration of 10 μ M was used subsequently, as it had no effect on proliferation. Taxol or nocodazole or FCF or DMSO (control) were added to the culture medium at 66 hours and myofibers were cultured for another 6 hours before harvesting and fixing in 4% PFA.

Immunofluorescence microscopy and imaging

Myofibers were permeabilized in 0.5% Triton X-100 (Sigma) in PBS for 6 minutes, washed in PBS 1X, and incubated in blocking solution (20% horse serum in PBS; GIBCO) for 30 minutes at RT. Primary antibodies in PBS were applied to fibers and fibers were incubated overnight at 4°C. Following 3 washes in 0.025% Tween20 in PBS (ACROS Organics), secondary antibodies diluted at 1:500 in PBS were applied and fibers were incubated for 1 hour at RT. Fibers were then mounted in Vectashield with Dapi (Vector labs) and images captured on a Zeiss ApoTome 2. All images were assembled in Adobe Photoshop. Antibodies are listed in Table S1.

Transmission electron microscopy

72-hour cultured myofibers were fixed in 4% PFA + 2.5% glutaraldehyde in PBS and embedded in Epon resin. Thin sections (85nm) were taken using a glass knife on an ultra-microtome (Leica UC6). Sections were collected on copper grids and electron micrographs were obtained from a transmission electron microscope FEI Tecnai G2 Blotwin at 120kv imaged by a Gatan Orius SC1000B digital camera.

References for Experimental Procedures

Sharma, N., Kosan, Z.A., Stallworth, J.E., Berbari, N.F., and Yoder, B.K. (2011). Soluble levels of cytosolic tubulin regulate ciliary length control. *Molecular biology of the cell* 22, 806-816.

Table S1: List of antibodies used in this study

| Primary antibodies | Type | Product code | Dilution | Provider |
|----------------------|-------------------|--------------|----------|--------------------------------------|
| PAX7 | Mouse monoclonal | Pax7 | 1:20 | Developmental Studies Hybridoma Bank |
| MYOGENIN | Mouse monoclonal | F5D | 1:50 | Developmental Studies Hybridoma Bank |
| MYOGENIN | Rabbit polyclonal | sc-576 | 1:60 | Santa Cruz Biotech |
| MYF5 | Rabbit polyclonal | sc-302 | 1:1000 | Santa Cruz Biotech |
| MYOD | Rabbit polyclonal | sc-304 | 1:2000 | Santa Cruz Biotech |
| M-CADHERIN | Goat polyclonal | sc-6470 | 1:250 | Santa Cruz Biotech |
| CAVEOLIN-1 | Rabbit polyclonal | sc-894 | 1:400 | Santa Cruz Biotech |
| ARL13B | Mouse monoclonal | 75-287 | 1:1000 | UC Davis/NIH NeuroMab Facility |
| GFP | Chick polyclonal | ab13970 | 1:600 | ABCam |
| Acetylated TUBULIN | Mouse monoclonal | T6793 | 1:300 | Sigma |
| Secondary antibodies | Type | Product code | Dilution | Provider |
| Alexa 594 anti-goat | Donkey | A11058 | 1:500 | Life Technologies |

| | | | | |
|-----------------------|-------------------|--------|-------|-------------------|
| | polyclonal | | | |
| Alexa 594 anti-mouse | Goat polyclonal | A11005 | 1:500 | Life Technologies |
| Alexa 488 anti-mouse | Donkey polyclonal | A21202 | 1:500 | Life Technologies |
| Alexa 488 anti-rabbit | Goat polyclonal | A11008 | 1:500 | Life Technologies |
| Alexa 633 anti-rabbit | Goat polyclonal | A21071 | 1:500 | Life Technologies |

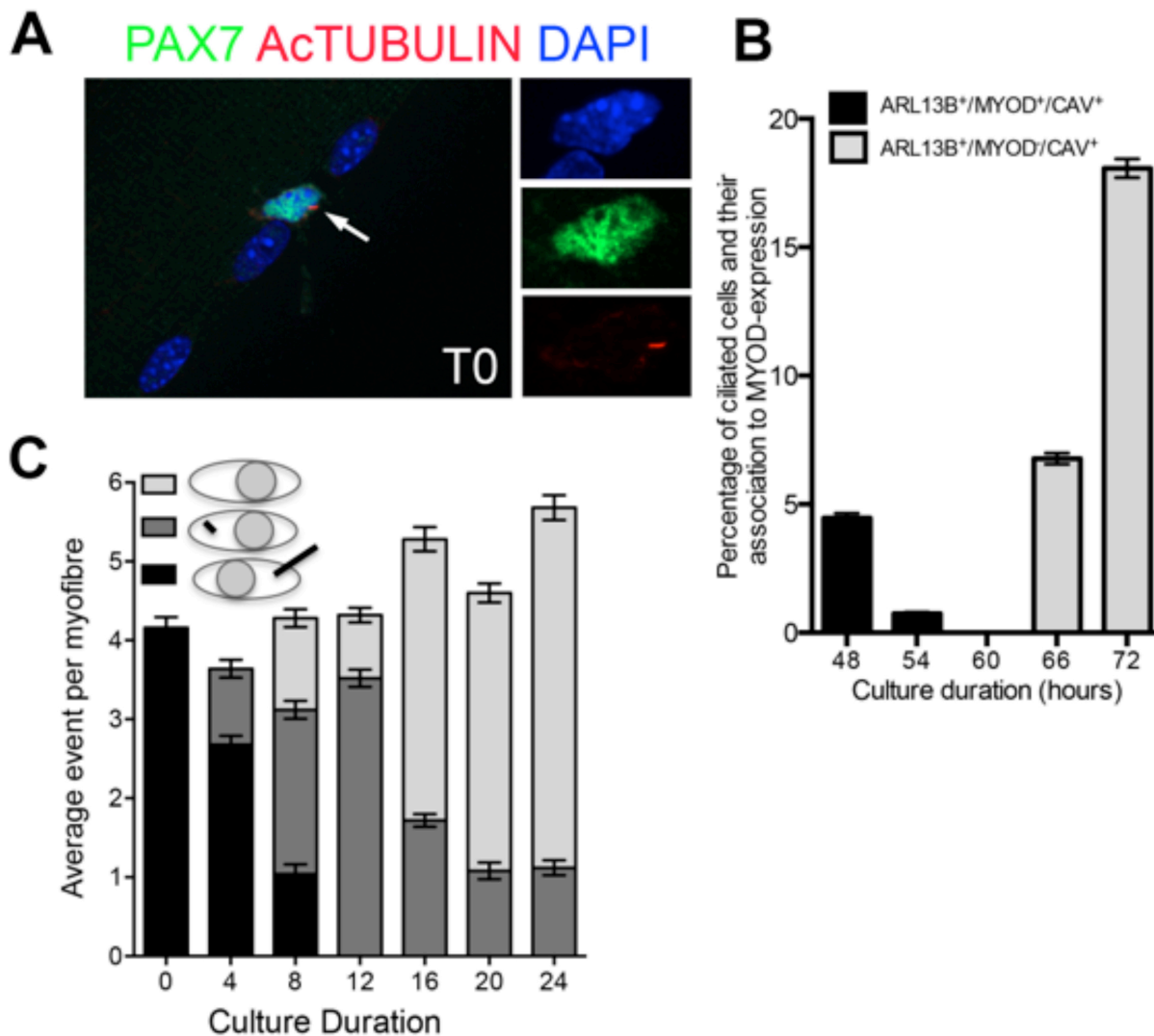


Figure S1. Primary cilia are disassembled as satellite cells enter proliferation and

differentiation. (A) Immuno-fluorescence characterization of primary cilia at the surface of quiescent SCs. Freshly isolated *Tg(Pax7-GFP)* myofibers were analysed by immunofluorescence using antibodies against GFP (green) and acetylated a TUBULIN (red). The white arrow indicates a primary cilium at the surface of a SC. (B) Time-course analysis of cilia resorption in the first 24 hours of myofiber culture. Cilia were recorded at 4-hour intervals according to their length as illustrated in the images and diagrams shown above the graph. $n = 50$ fibres from 3 independent experiments; mean \pm sem is shown. (C) Time-course analysis of cilia resorption in transit amplifying cells expressing MYOD between 48 and 72 hours. Myofibers were harvested at 6-hour intervals. $n = 50$ fibres per time point from 3 independent experiments; mean \pm sem is shown.

Related to Figure 1.